

Drastic changes in the molecular absorption at redshift $z = 0.89$ toward the quasar PKS 1830–211

Muller S.¹ and Guélin M.^{2,3}

¹ Academia Sinica Institute of Astronomy and Astrophysics (ASIAA), P.O. Box 23–141, Taipei, 106, Taiwan

² Institut de Radio Astronomie Millimétrique (IRAM), 300 rue de la piscine, F–38406 St Martin d’Hères,

³ Ecole Normale Supérieure/LERMA, 24 rue Lohmond, F–75005 Paris, France

Received 16 June 2008 / Accepted 24 September 2008

ABSTRACT

A 12 year-long monitoring of the absorption caused by a $z = 0.89$ spiral galaxy on the line of sight to the radio-loud gravitationally lensed quasar PKS 1830–211 reveals spectacular changes in the HCO^+ and HCN (2-1) line profiles. The depth of the absorption toward the quasar NE image increased by a factor of ~ 3 in 1998-1999 and subsequently decreased by a factor ≥ 6 between 2003 and 2006. These changes were echoed by similar variations in the absorption line wings toward the SW image. Most likely, these variations result from a motion of the quasar images with respect to the foreground galaxy, which could be due to a sporadic ejection of bright plasmons by the background quasar. VLBA observations have shown that the separation between the NE and SW images changed in 1997 by as much as 0.2 mas within a few months. Assuming that motions of similar amplitude occurred in 1999 and 2003, we argue that the clouds responsible for the NE absorption and the broad wings of the SW absorption should be sparse and have characteristic sizes of 0.5 – 1 pc.

Key words. Quasars: individual: PKS 1830–211 – Quasars: absorption lines – Galaxies: ISM – ISM: molecules

1. Introduction

Atomic and molecular line absorption measurements against bright sources are a powerful tool for studying the chemical composition and structure of the interstellar gas. In the cases where very small structures are present and where, due to proper motions, the line of sight scans across these structures, the absorption profile may vary with time. Such time variations allow the cloud properties to be studied on scales hardly accessible to other techniques.

Time variations of Galactic HI 21-cm line absorptions have been reported on the line of sight to pulsars by Frail et al. (1994), but were not reproduced by later studies (e.g., Stanimirović et al. 2003). Brogan et al. (2005) find temporal variations of the HI line absorption on the line of sight of the quasar 3C 138 over a 7-yr time span, although only out of three epochs of data. Time variations have also been observed for optical atomic lines toward bright stars [see a review in Crawford 2003]. Typically, these variations have amplitudes of 10% or less and time scales of several months or years. They are interpreted as the signature of structures as small as 10 – 100 astronomical units (AU) in the Galactic interstellar medium (ISM). Evidence of such small structures comes from VLBI absorption measurements against closely packed continuum sources (Dieter et al. 1976; Diamond et al. 1989; Faison & Goss 2001). Most likely, they are clumps or filaments expelled by supernova explosions or stellar winds.

As for molecular gas, variations have been detected in centimeter-wave absorption spectra of H_2CO (Marscher et al. 1993) and OH (Moore & Marscher 1995),

in millimeter-wave spectra of HCO^+ (Liszt & Lucas 2000) and in optical spectra of CH, CH^+ and CN (Pan et al. 2001; Rollinde et al. 2003). Here also, the absorption occurs in Galactic diffuse clouds seen against bright stars or quasars. The variations are observed over periods > 1 yr and their amplitude is seldom above 10%. They arise from 10 – 100 AU size structures of the Galactic ISM similar to those observed in the atomic lines.

There are less data concerning absorption variations in extragalactic clouds. Time variability of HI line absorption has been reported at $z = 0.52$ (Wolfe et al. 1982), $z = 0.31$ (Kanekar & Chengalur 2001) and $z = 0.67$ (Kanekar & Chengalur 2008) in front of radio quasars. The short time scales, on the order of a few days for the first two studies, may be explained by interstellar scintillation coupled with parsec or sub-parsec scale structures in the absorbing galaxies.

Wiklind & Combes (1997) also report time variations in the CO absorption profile observed against the quasar PKS 1413+135 at a redshift $z = 0.25$. The absorption occurs in the host galaxy, which is seen almost edge-on, and the variations primarily affect the nearly saturated absorption peak, the intensity of which was found to decrease over two years. Wiklind & Combes (1997) interpret these variations by structural changes in the background continuum source, resulting in a changing line of sight through the absorbing gas. The latter consists of small dense clumps embedded in a mostly diffuse medium.

In this article, we report the detection of large variations in the HCO^+ and HCN absorption profiles observed at $z = 0.89$ on the line of sight to the quasar PKS 1830–211. PKS 1830–211 is a radio-loud quasar at a redshift of

$z = 2.5$ (Lidman et al. 1999), whose line of sight is intercepted by a spiral galaxy (Winn et al. 2002) at a redshift $z = 0.88582$ (Wiklind & Combes 1996). The galaxy gives rise to absorption in many molecular lines (see, e.g., Wiklind & Combes (1998); Muller et al. (2006) –hereafter MGD– and references therein) and acts as a gravitational lens. At millimeter wavelengths, the image of the quasar is split into two compact continuum sources (denoted NE and SW images), separated by $1''$, or $\simeq 8$ kpc, and they appear on opposite sides of the galaxy bulge. At $\lambda = 3$ mm, the NE image contributes about $2/3$ of the total continuum flux and the SW image the remaining $1/3$, a ratio that fluctuates in relation to background source flux variations (van Ommen et al. 1995; Wiklind & Combes 1999) coupled with a time delay of about 25 days (Lovell et al. 1998; Wiklind & Combes 1999).

This peculiar configuration makes it possible to explore along two pencil beams the chemical composition and structure of the gas. Absorption is most prominent in the $J = 2 - 1$ lines of HCO^+ and HCN, both of which show two distinct absorption components: *i*) a broad component (FWZP $\Delta V = 100 \text{ km s}^{-1}$) around $V = 0 \text{ km s}^{-1}$ ¹, associated with the SW image, which is obviously saturated and presumably consists of several distinct clouds, and *ii*) a narrow component ($\Delta V \sim 15 \text{ km s}^{-1}$), 146 km s^{-1} lower in velocity and associated with the NE image. Both components were found to vary in intensity and shape in the course of a 12 year-long monitoring of the quasar. The amplitude of the variations, the duration of the monitoring period and the redshift of the absorbing system offer a rare opportunity to investigate the gas properties in the arms of a relatively young spiral galaxy.

2. Observations

The observations discussed in this paper concern the HCO^+ and HCN ($J = 2 - 1$) lines, redshifted by 0.88582 to ~ 94 GHz, whose absorption profiles were monitored over the period September 1995 – May 2007. They were carried out with the IRAM Plateau de Bure interferometer (PdBI) or the IRAM 30m telescope.

The PdBI data were mostly taken with the array in a compact configuration, often in average weather conditions, in the frame of an observing program whose goal was to measure isotopic abundance ratios in the lensing galaxy (MGD). The strong flux of PKS 1830–211 ($\simeq 2 \text{ Jy}$ at $\lambda = 3$ mm) allowed us to self-calibrate the spectra with respect to the continuum emission, so that accurate absorption profiles, normalized to the continuum, could be derived even under marginal atmospheric phase stability. The calibration accuracy on the normalized PdBI spectra is better than a percent of the continuum level. The HCO^+ (2-1) spectra obtained with the PdBI in the period 1995 – 2007, normalized to the total (NE+SW) continuum flux, are displayed on Fig.1. The integration time for each individual spectrum ranged from 0.5 to 3 hours and the signal-to-noise ratio is generally excellent.

Additional HCO^+ (2-1) spectra were observed between 1996 and 1999 by T. Wiklind and F. Combes with the IRAM 30-m telescope. They were part of a program aiming to measure the Hubble constant H_0 using the variability of the quasar and the geometrical time delay between the two

gravitationally lensed images. As it is difficult to concisely show all (~ 60) the HCO^+ (2-1) 30-m telescope spectra, we have shown in Fig.1 only 3 spectra obtained at critical periods: Aug 1996, Oct 1997 and Jan 1999. The rest of the 30-m HCO^+ data are displayed in the form of flux and the integrated line opacity data points (see below). A list of all the observations is given in Table 1.

Finally, we collected 4 HCN (2-1) spectra, 3 observed with the PdBI and 1 with the 30-m telescope. They are shown on Fig.2. We note that, since 2007, the HCN spectra were observed simultaneously with the HCO^+ , thanks to the new broad-band dual-polarization receivers installed at the PdBI.

Difference spectra of 13 of the HCO^+ (2-1) spectra, re-sampled and smoothed to a velocity resolution of 5 km s^{-1} , are shown on Fig.3. They clearly illustrate the drastic changes that affected the absorption profile between 1998 and 2004.

In total, the available data densely cover a 12 year-long period, except for breaks in 1998 and between 2003 and 2006. At each daily session, the flux of PKS 1830–211 was derived from the observation of a strong reference source (3C 273, 3C 345, 1749+096, or MWC 349), whose flux is regularly monitored with IRAM instruments. These flux measurements are reported in Fig.4a. We estimate that the continuum flux of PKS 1830–211 should be accurate to 15% (r.m.s.).

Whereas the knowledge of the NE/SW flux ratio is crucial for the derivation of line opacities, the low angular resolution of all but the PdBI 2003 observations made it generally impossible to resolve the NE from the SW image. Nevertheless, the NE/SW continuum flux ratio could accurately be derived from the depth of the HCO^+ and/or HCN (2-1) absorption trough around 0 km s^{-1} , where the profiles are heavily saturated (see MGD). Since the absorbing gas is very cold with respect to the hot non-thermal background source, and since the NE source is free of absorption at this velocity, the signal detected at 0 km s^{-1} simply reflects the flux of the NE continuum source. We report the evolution of the flux ratio NE/SW in Fig.4b.

3. Results

The most striking result in Fig.1 is the change in intensity of the -146 km s^{-1} absorption feature that occurred around 1998 and 2004. The depth of this feature, which in 1995-1996 amounted to $\simeq 7\%$ of the total continuum (and 11% of the NE continuum source), increased by 1999 to 20% (32% of the NE continuum source) and dropped almost to zero ($\leq 5\%$) sometime between 2003 and 2006 – a drastic change observed in both HCO^+ and HCN (2-1) (see Fig.2).

The changes in the NE image absorption are echoed in the SW image by parallel changes of the blue absorption wing (i.e., $V \in [-50, -15] \text{ km s}^{-1}$) as can be seen in Fig.3 and Fig.5. In contrast, the flat absorption trough at $V \in [-7, +12] \text{ km s}^{-1}$ shows only small intensity variations (Fig.4b).

The major changes are observed on a time scale of 2 to 3 years. In contrast, the variations of the absorption trough near 0 km s^{-1} , which typically reach $\simeq \pm 20\%$ of the SW source flux (see Fig. 4), have much shorter time scales: less than 2 months. As mentioned above, they mostly reflect variations in the NE/SW source flux ratio, caused by the difference in path lengths between the NE and the

¹ We adopt a heliocentric reference frame.

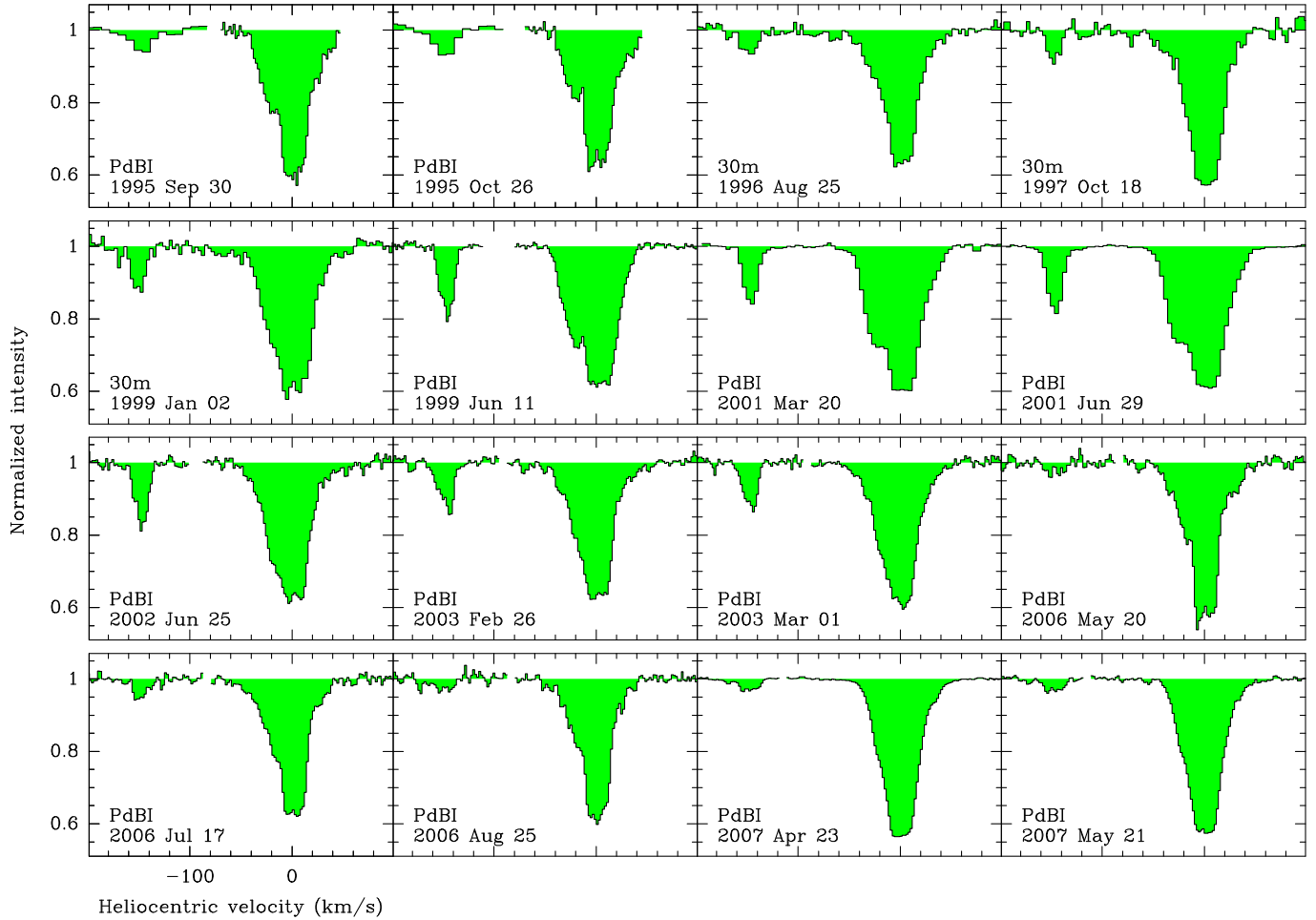


Fig. 1. Spectra of the HCO^+ absorption toward PKS 1830–211, obtained either with the PdBI or the 30m, at different epochs between 1995 and 2007. The intensity is normalized with respect to the total (NE+SW) continuum flux. The velocity resolution is 2 km s^{-1} , except for the spectral window on the -146 km s^{-1} component in 1995, where it is 8 km s^{-1} , for 2001 spectra, where it is 4 km s^{-1} , and for 30m spectra, where it is 3 km s^{-1} .

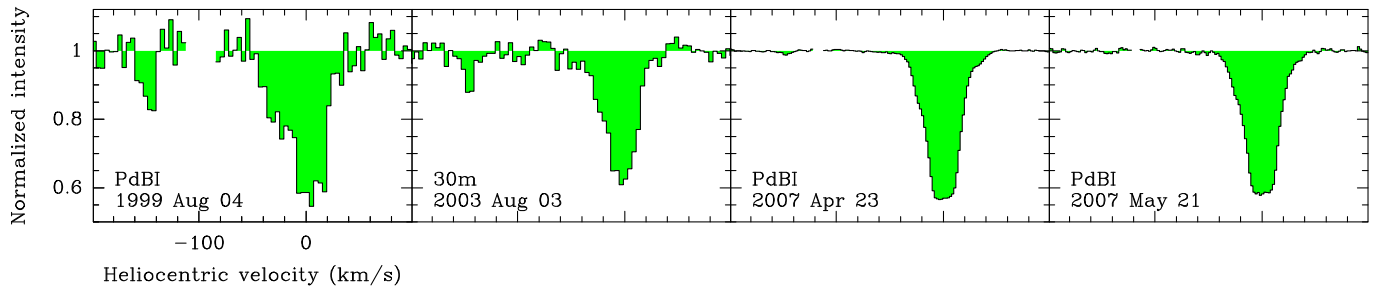


Fig. 2. Spectra of the HCN (2-1) absorption toward PKS 1830–211 at different epochs between 1999 and 2007. The velocity resolution is 4 km s^{-1} for 1999 and 2003 spectra and 2 km s^{-1} for 2007 spectra.

SW images (Lovell et al. 1998; Wiklind & Combes 1999), variations which tend to be smeared out after a few months.

Whereas the short term variations of the absorption near 0 km s^{-1} are caused by sudden flux variations of the background quasar, coupled to the propagation delay just mentioned, the reason for the large long term variations are less clear.

We first note that the destruction (or formation) of the HCO^+ and HCN molecules on time scales of months are out of question in view of the large extent of the absorbing cloud(s) that we derive below ($\sim 1 \text{ pc}$). For the same reason,

significant changes of the HCO^+ and HCN line excitation temperature can be ruled out.

To explain the growth of the -146 km s^{-1} absorption feature in 1998-1999 and its fade-out in 2006-2007, we have to involve either *a*) a motion of the clouds causing the -146 km s^{-1} absorption with respect to the background continuum source, *b*) a micro-lensing event in the spiral galaxy, or *c*) the appearance/disappearance of a bright spot in the quasar.

The monitoring of the total flux and flux ratio (Fig.4) is instructive in this respect. The total flux first increased

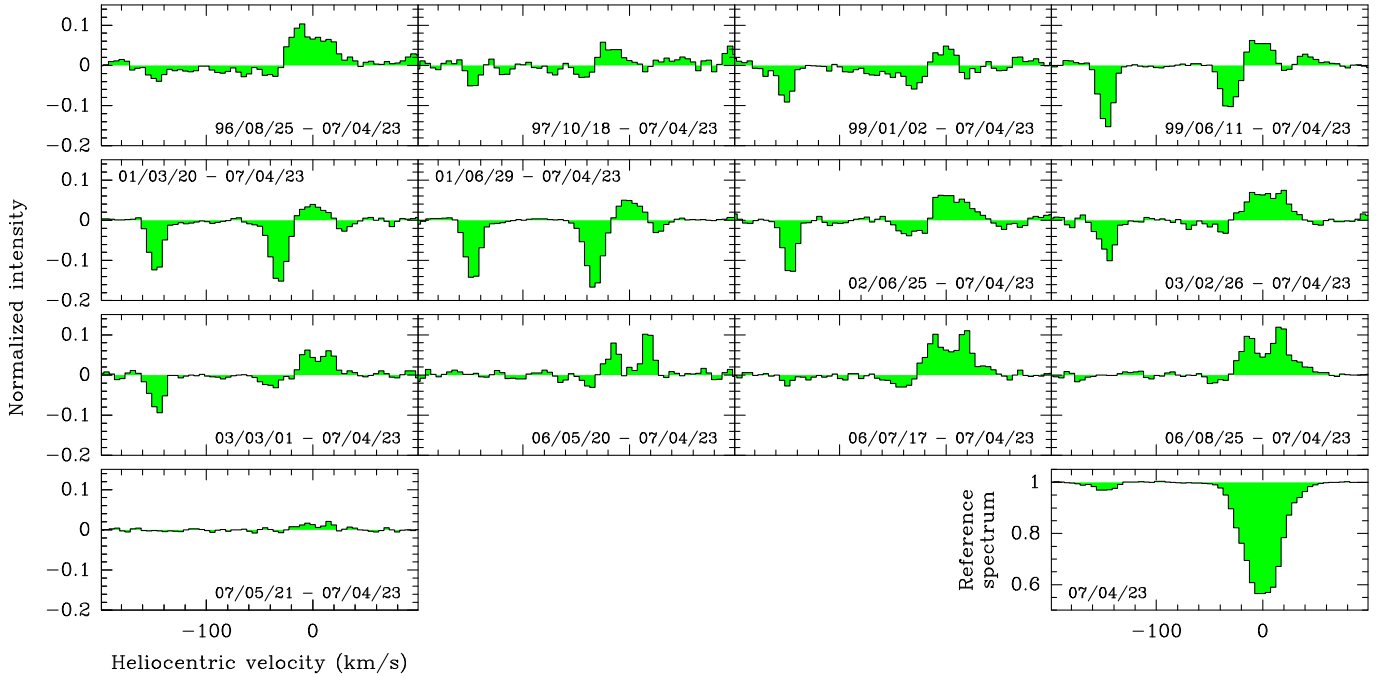


Fig. 3. Difference spectra for the HCO^+ (2-1) line. The reference spectrum is that of 2007 Apr 23 (*bottom right*). The date format is yy/mm/dd. Spectra were resampled and smoothed to a velocity resolution of 5 km s^{-1} .

from 1 Jy to 2 Jy between 1997 and mid-1999, stood well above 2 Jy for a period of 2–3 yr, and decreased from 2.5 Jy to 1.5 Jy between 2002 and 2003. These flux changes are in phase with the absorption changes just described, which seems hardly compatible with a simple motion of the clouds with respect to the source as in *a*). By 2007, the total flux has recovered its 2001 value of 2.5–3 Jy, whereas the -146 km s^{-1} absorption feature has remained vanishingly weak. We note that Lewis & Ibata (2003) have tentatively interpreted absorption-line variations in terms of micro-lensing. However, the good correlation between the NE -146 km s^{-1} and the SW -20 km s^{-1} blue wing absorption variations, plus the relatively stable value of the flux ratio over 1996–2007, seem to rule out micro-lensing events as in *b*). The most likely cause of the absorption variations seems thus to be *c*), the recurrent emission/disappearance of bright emission blobs in the quasar.

4. Discussion

4.1. The continuum source size

The structure of PKS 1830–211 has been studied with VLBA interferometry at frequencies of up to 43 GHz (see Jin et al. 2003 and references therein). At 43 GHz, the continuum emission reduces to two compact sources of similar sizes, the NE and SW images, plus two arc-like features that are the remnants of the Einstein ring observed at longer wavelengths. The compact sources probably image the optically thick radio core of the blazar and the arclets, the jet. The arclet emission has a steeper spectral index than the core emission and its flux at 43 GHz is already 10 times lower than the core flux. It should thus become negligible at the frequency of our observations (94 GHz). Jin et al. (2003) marginally resolve the core images at 43 GHz with a 0.5 mas synthesized beam and find, for the NE core, a size of $\approx 230 \times 150 \mu\text{as}$ that corresponds to $1.8 \times 1.2 \text{ pc}$ in the plane

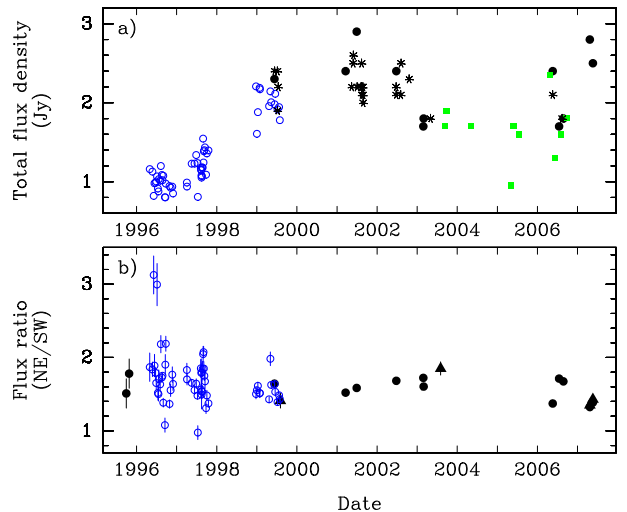


Fig. 4. **a)** Evolution of the total continuum flux density (NE+SW) of PKS 1830–211 at frequencies $\sim 94 \text{ GHz}$. Open circles: 30-m measurements at the frequency of the redshifted HCO^+ (2-1) line; filled circles: same for PdBI measurements; asterisks: PdBI measurements at frequencies between 91 and 104 GHz; triangles: PdBI measurements for HCN (2-1); squares: flux measurements with the Australian Telescope Compact Array (from the webpage: <http://www.narrabri.atnf.csiro.au/calibrators/>) at various frequencies between 89 and 96 GHz. **b)** Evolution of the flux ratio NE/SW, as derived from the average depth of the absorption between -7 and $+12 \text{ km s}^{-1}$, where the signal represents the continuum flux of the NE source (see text).

of the $z = 0.89$ galaxy (assuming a flat Universe with the standard cosmology parameters: $H_0 = 70 \text{ km s}^{-1} \text{ Mpc}^{-1}$, $\Omega_M = 0.3$ and $\Omega_\Lambda = 0.7$). According to VLBI data, the core

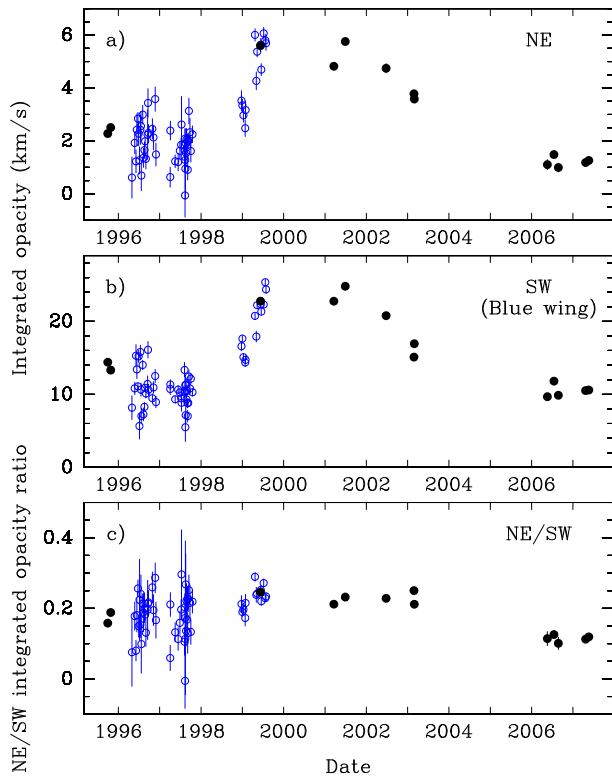


Fig. 5. Variations of **a)** the integrated opacity of the NE absorption component (integrated between -160 and -130 km s^{-1}), **b)** the integrated opacity of the blue wing of the SW component (integrated between -50 and -15 km s^{-1}), and **c)** the ratio of the two previous quantities. Open circles correspond to 30m data and filled circles to PdBI observations. See Table 1.

image scales almost linearly in size with wavelength, as expected for a self-absorbed synchrotron source. Therefore, at 94 GHz, its diameter should be $0.5 - 1$ pc.

4.2. The absorbing clouds in front of the NE source

The -146 km s^{-1} HCO^+ (2-1) absorption reached a depth of $\sim 20\%$ of the total continuum in 1999, when the flux of the NE image was 62% of the total flux. This, and the VLBA core size measurements, set strong constraints on the peak optical depth τ_0 , as well as on the source filling factor f_c and absorbing cloud sizes.

We have:

$$\tau_0 = -\ln \left[1 - \frac{I_0 - I_A}{f_c I_{NE}} \right], \quad (1)$$

where I_0 is the continuum level ($I_0 = 1$ for the normalized spectra), $(I_0 - I_A)$ the apparent depth of the absorption for the -146 km s^{-1} feature ($= 0.2I_0$), and $I_{NE} = 0.62I_0$ the NE image continuum flux. Taking into account that $f_c \leq 1$ and $\tau \leq \infty$, we find from Eq.[1] that $\tau_0 \geq 0.4$ and $f_c \geq 1/3$. Thus, in 1999, the absorbing material was covering at least one-third of the NE image.

MGD noted a great similarity in the shapes of the -146 km s^{-1} absorption feature in HCO^+ and HNC , despite the 4 times weaker intensity of the HNC feature. This similarity, and the non-detection of the -146 km s^{-1} feature in H^{13}CO^+ , down to a level 50 times lower than HCO^+ ,

probably means that the clouds responsible for the NE absorption cannot be optically thick. Adopting this view, we find $\tau_0 \simeq 0.4$ and $f_c \simeq 1$.

How many clouds are actually responsible for the absorption of the NE core and what can we learn about them? Obviously, the number ought to be small, judging from large amplitude of the opacity variations, as well as from the shape of the absorption profile.

We have fitted the profiles of the -146 km s^{-1} feature, observed at different epoch, with Gaussians. Within the noise, all profiles can be fitted with 3 Gaussians of HPW $5 - 8$ km s^{-1} , respectively. Following Marscher & Stone (1994), we have also carried out a statistical analysis of the profile variations assuming a random distribution of absorbing clouds. The clouds are assumed to have identical column densities, but a size spectrum $dN/dL \propto L^{-(D+1)}$, where we adopted for the fractal dimension $D = 1.5$. Within the limits of this exercise (limited period of monitoring, integration over the extent of the continuum sources, and, mostly, scarcity of information on the motion of these sources, as will be seen below), we find that the observed large opacity variations imply a small number of absorbing clouds, N_{abs} . More specifically, we find in the framework of Marscher & Stone's model that the expected fractional change in equivalent width, $\langle \delta W \rangle / \langle W \rangle$ exceeds 50% only for $N_{abs} \leq 5$ ². Then, the clouds responsible for the bulk of the absorption should not be much smaller than the size of the background continuum source, ~ 1 pc. Of course, this simple analysis is biased against structures much smaller than the continuum sources and we cannot rule out the presence of small cloudlets whose cumulative contribution would be a small fraction of the absorption.

From the observation of two different rotational transitions, Wiklind & Combes (1996) and Carilli et al. (1998) derived rotation temperatures T_{rot} for CS, H^{13}CO^+ , H_2CO and N_2H^+ (and upper limits to those of H^{12}CO^+ and HCN) close to (slightly higher than) the expected cosmic background radiation temperature, $T_{CBBR} = 5.1$ K at $z = 0.89$, implying that the average gas density is $< 10^5$ cm^{-3} . Unfortunately, the first 3 rotational transitions of CO are unobservable from the ground, and only the $J = 4-3$ line has been so far detected (Wiklind & Combes 1998; Gérin et al. 1997), so we do not know the rotation temperature of this low dipole moment species and cannot set a more constraining upper limit to the gas density. In any case, all multi-transition observations have been made toward the SW source, where absorption is stronger, and there is no direct constraint on the gas density toward the NE source.

The CBR temperature, however, is high enough to populate the HCO^+ $J = 1$ level ($E/k = 4.3$ K) without the help of collisions. At radiative equilibrium, the HCO^+ $J = 2 - 1$ line opacity becomes $\simeq 0.4$ as soon as the HCO^+ column density per km s^{-1} reaches $dN/dv = 10^{12}$ cm^{-2} km s^{-1} , i.e. the H column density $N(\text{H})$ exceeds a few $\times 10^{21}$ cm^{-2} , assuming the fractional HCO^+ abundance is similar to that in diffuse Galactic clouds (2×10^{-9} , according to Liszt & Lucas 2000). For a cloud depth of 1 pc, the gas density in the NE absorbing clouds would be $n(\text{H}) = \text{few} \times 10^2$ cm^{-3} and the visual extinction per cloud,

² This number was derived from equation (7) of Marscher & Stone (1994), after correction of a typographical error on the last exponent, which should read $n + i - 1$ instead of n

presumably, $A_v \sim 1$ mag, if the dust properties are similar to those in the vicinity of the Sun: the absorbing cloud(s) look very much alike the local Galactic diffuse clouds.

In the case of PKS 1413+135, Wiklind & Combes (1997) find excitation temperatures for the $J = 1 - 0$, $2 - 1$ and $3 - 2$ lines significantly higher than the 3.4 K CBR temperature at $z = 0.25$, and which seem to increase with increasing J . They interpret their data as evidence of at least two gas components along the line of sight, one of which could be in the form of dense clumps. However, the line of sight to PKS 1413+135 crosses a much larger fraction of the molecular disk than in the case of PKS 1830–211, since the galaxy is seen almost edge-on, and the solid angle subtended by the continuum source is probably smaller, since PKS 1413+135 is not magnified, two conditions that may enhance the visibility of small clumps.

4.3. Variability of the continuum source

The variations in the absorption profiles cannot be caused by the proper motion of the $z = 0.89$ galaxy with respect to the observer. Indeed, the apparent drift of the clouds with respect to the continuum source is:

$$s = V_{\perp} \Delta t / (1 + z_{abs}), \quad (2)$$

where V_{\perp} is the transverse velocity and Δt the time interval in the Earth frame, for which we apply the relativistic correction for the time dilation measure at the redshift z_{abs} of the galaxy. With $V_{\perp} \sim 1000$ km s $^{-1}$ and on time scales of about a year, $s \sim 100$ AU, i.e., 3 orders of magnitude smaller than the extent of the clouds derived above (≥ 0.5 pc).

Whereas the observer, the absorbing clouds and the background galaxy that host the quasar should have relative velocities $\lesssim 1000$ km s $^{-1}$, the images of the radio core, which consists of plasmons, can move arbitrarily fast, provided the geometry is favorable. VLBA measurements at 43 GHz show variations in the apparent separation between the NE and SW cores on time scales of only months. Early in 1997, Jin et al. (2003) measured this parameter 8 times at intervals of 14 days or so. These authors found that the NE core source moved with respect to its SW counterpart by as much as $\simeq 140$ μ as in 4 months. A comparison with previous data, obtained 8 months earlier, showed a change ~ 200 μ as in the opposite direction. This is about the extent of the continuum cores at 43 GHz and twice their expected extent at 94 GHz. Projected on the plane of the lensing galaxy, 200 μ as corresponds to ~ 1.6 pc. We note that the relative displacement of the NE and SW sources implies an apparent velocity of $v \sim 8c$ in this plane, so that the source/observer geometry should indeed be particularly favorable. There are more high frequency data on PKS 1830–211 in the VLBA archive. Once calibrated, they may teach us about the motion of the continuum sources throughout our monitoring period. This will be the object of a subsequent study.

Nair et al. (2005) interpret the apparent motion of the NE and SW sources by the recurrent ejection of plasmons along a helical jet. The plasmons are ejected at relativistic velocities by a precessing "nozzle" pointing toward the observer. The plasmons appear as bright self-absorbed synchrotron sources and remain visible at millimeter wavelengths for a few months. Traces of fading plasmons may

have been observed by Garrett et al. (1997) in July 1996 at 43 GHz, in the form of compact emission "knots" located close to the bright NE and SW cores. These knots had vanished by January 1997, when Jin et al. (2003) resumed VLBA observations. Unfortunately, there is no higher frequency data allowing us to zoom deeper into the barely resolved cores.

We have noted above the good correlation between the opacity variations of the -146 km s $^{-1}$ NE and -30 km s $^{-1}$ SW absorption components on Fig.5. Obviously, these components are two clouds observed against the NE and SW images of the same plasmon. That both components increased and faded out at the same time (within the coarse sampling of our observations) may mean that the bright plasmon responsible of the bulk of the absorption at these velocities appeared in 1999 and faded out in 2003. The total flux variations (Fig.4a) seem to corroborate this picture. The new increase of the continuum flux in 2007, which seems to have not affected the absorption profiles, could be due to the appearance of a new plasmon in a direction free of any cloud.

4.4. The nature of the optically thick absorption component toward the SW source

As pointed out by several authors, the wide range of velocities ($\simeq 100$ km s $^{-1}$) over which absorption is seen toward the SW core image is puzzling: the spiral galaxy appears almost face-on in the HST optical images, and the SW core source is very small (~ 1 pc). How can such a large span of velocities be reached over such a small region? According to gravitational lens models of PKS 1830–211 (e.g. Nair et al. 1993), the SW core source image lies 2–3 kpc away from the galactic nucleus, so that no large velocity gradient is expected over an area of a few pc. Could the absorptions near/below -30 km s $^{-1}$ and above $+30$ km s $^{-1}$ come from a distinct, more extended continuum source filtered out in the VLBI observations? Probably not, as there is no trace of such a source on the VLA 47 GHz maps of Carilli et al. (1998). Moreover, the HCO $^+$ $J = 2 - 1$ observations of MGD in the PdBI extended configuration show that the absorption in the SW component wings arises within ~ 1 kpc from the SW core source.

The width of the absorption and the detection toward the SW source of very rare isotopologues such as HC 17 O $^+$ and HC 15 N imply molecular column densities and masses characteristic of large Galactic molecular clouds: H $_2$ column density of 3×10^{23} cm $^{-2}$ and molecular gas mass integrated over 1 square parsec of $\simeq 5 \times 10^3$ M $_{\odot}$, if we assume fractional abundances relative to H $_2$ of 10^{-9} for HCN and HCO $^+$ and 10^{-7} for OH (see MGD and Liszt & Lucas 1999). We note that the H $_2$ column density we adopt is higher than those derived by Wiklind & Combes (1998) and Gérin et al. (1997) from CO(4-3) observations. However, the high energy of the CO $J=4$ level ($E/k = 56$ K) and the rather low signal-to-noise ratio of the CO spectra make the latter column densities fairly uncertain. Even so, the very broad absorption is more reminiscent of the Galactic Center clouds (e.g., Christopher et al. 2005) or of exceptional Giant Molecular Clouds such as W49A-N (Williams et al. 2004) than of the more common molecular clouds scattered in the arms of the Galactic disk. Is the model of the lensing galaxy inaccurate and could the SW source be closer to the center of the $z = 0.89$ galaxy? Higher

angular resolution observations of the $\text{HCO}^+ J = 2 - 1$ absorption would be warranted to solve this question.

We address a final point concerning the implication of the time variations for our previously published study of isotopic abundance ratios in the $z = 0.89$ galaxy (MGD). The sole reason for us to monitor the HCO^+ (2-1) absorption profile was to check for changes in the NE/SW flux ratio that could have biased the interpretation of our measurements. Fortunately, no significant changes seem to have occurred between 1999 and 2001, when most of our data on rare isotopes were taken. The $\text{H}_2^{32}\text{S}/\text{H}_2^{34}\text{S}$ ratio ($= 10.6 \pm 0.9$) was measured later in 2005-2006, but the lines of both isotopologues are close in frequency and were observed simultaneously. The new PdBI receivers, with larger bandwidth and flexible correlator setting, now allow us to simultaneously observe lines distant in frequency by as much as 4 GHz. This is the case for example for the $J = 2-1$ lines of H^{13}CO^+ , HC^{18}O^+ and HC^{17}O^+ in sources like PKS 1830–211 or B 0218+357 (Muller et al., in prep.).

5. Conclusions

Our monitoring of the absorption at $z = 0.89$ on the line of sight to the quasar PKS 1830–211 has revealed spectacular changes in the HCO^+ and HCN (2-1) line profiles on time scales of about a year. These primarily concern the absorption toward the quasar NE image, which increased by a factor of $\simeq 3$ between 1996 and 1999 and decreased by a factor ≥ 6 between 2003 and 2006. They also concern the broad absorption wings observed toward the SW image.

We interpret the large absorption variations as resulting from the appearance/disappearance of discrete components in the background continuum source. Indeed, the good correlation between the opacity variations toward the NE and the SW images seem to rule out micro-lensing events. The continuum source most likely consists of bright plasmons sporadically ejected at relativistic velocities, a motion magnified by the gravitational lens. The separation between the NE and SW continuum images has been found to vary between 1996 and 1997 by ~ 0.2 mas from VLBA observations. Assuming that a motion of similar amplitude occurred in 2003, the size of the continuum images, the depth of the absorption, and the near disappearance of the NE absorption feature since 2006 teach us that the absorbing clouds toward the NE source should be: *a)* sparse, as otherwise the variations would be less pronounced, *b)* compact, as they must have covered at some point most of the 1 pc continuum image and *c)* have sizes covering a good fraction of a pc. It is likely that these clouds are diffuse clouds. The clouds which are origin of the saturated absorption toward the SW source, on the other hand, are much more massive and should be part of a Giant Molecular Cloud complex.

So far, there have been no VLBI observations of the HCO^+ and/or HCN line absorptions. Such observations at a resolution ≤ 0.1 mas would help to clarify the morphology of the clouds and may explain why the absorption toward the SW image is so extended in velocity. If the strong absorption changes observed in 1999 and 2003 are recurrent, coupled millimeter-wave absorption measurements and mm-VLBI continuum observations may help to better constrain the density and sizes of the molecular clouds in the $z = 0.89$ galaxy, stressing the potential of molecular absorption for the exploration of the interstellar medium in distant objects.

Acknowledgements. We would like to thank F. Combes and T. Wiklind for kindly communicating us their 30-m telescope data. We also thank F. Combes, H. Liszt and G. Henri for helpful discussions and the PdBI Observatory staff and IRAM-Grenoble SOG for their support in the observations. We acknowledge the referee for giving helpful and constructive comments. MG would like to thank the Taiwanese National Science Council for its support during a stay in ASIAA. Based on observations carried out with the IRAM Plateau de Bure Interferometer. IRAM is supported by INSU/CNRS (France), MPG (Germany) and IGN (Spain).

References

- Brogan, C. L., Zauderer, B. A., Lazio, T. J., et al., 2005, *AJ*, 130, 698
 Carilli, C. L., Menten, K. M., Reid, M. J., et al., 1998, *astro-ph/9801157*
 Christopher, M. H., Scoville, N. Z., Stolovy, S. R. & Yun, M. S., 2005, *ApJ*, 622, 346
 Crawford, I. A., 2003, *Ap&SS*, 285, 661
 Diamond, P. J., Goss, W. M., Romney, J. D., et al., 1989, *ApJ*, 347, 302
 Dieter, N. H., Welch, W. J. & Romney, J. D., 1976, *ApJ*, 206, L113
 Faison, M. D. & Goss, W. M., 2001, *AJ*, 121, 2706
 Frail, D. A., Weisberg, J. M., Cordes, J. M. & Mathers, C., 1994, *ApJ*, 436, 144
 Garrett, M. A., Nair, S., Porcas, R. W. & Patnaik, A. R., 1997, *Vistas in Astronomy*, 41, 281
 Gérin, M., Phillips, T. G., Benford, D. J., et al., 1997, *ApJ*, 488, L34
 Jin, C., Garrett, M. A., Nair, S., et al., 2003, *MNRAS*, 340, 1309
 Kanekar, N. & Chengalur, J. N., 2001, *MNRAS*, 325, 631
 Kanekar, N. & Chengalur, J. N., 2002, *A&A*, 381, L73
 Kanekar, N. & Chengalur, J. N., 2008, *MNRAS*, 384, L6
 Lewis, G. F. & Ibata, R. A., 2003, *MNRAS*, 340, 562
 Lidman, C., Courbin, F., Meylan, G., 1999, *ApJ*, 514, L57
 Liszt, H. & Lucas, R., 1999, in *Highly Redshifted Radio Lines*, eds. Carilli, C. L., Radford, S. J. E., Menten, K. M. & Langston, G. I., *ASP Conf. Ser.*, 156, 188
 Liszt, H. & Lucas, R., 2000, *A&A*, 355, 333
 Lovell, J. E. J., Jauncey, D. L., Reynolds, J. E., et al., 1998, *ApJ*, 508, L51
 Marscher, A. P., Moore, E. M. & Bania, T. M., 1993, *ApJ*, 419, 101
 Marscher, A. P. & Stone, A. L., 1994, *ApJ*, 433, 705
 Moore, E. M. & Marscher, A. P., 1995, *ApJ*, 452, 671
 Muller, S., Guélin, M., Dumke, M., et al., 2006, *A&A*, 458, 417 (MGD)
 Nair, S., Narasimaha, D. & Rao, A. P., 1993, *ApJ*, 407, 46
 Nair, S., Jin, C. & Garrett, M. A., 2005, *MNRAS*, 362, 1157
 Pan, K., Federman, S. R. & Welty, D. E., 2001, *ApJ*, 558, L105
 Rollinde, E., Boissé, P., Federman, S. R. & Pan, K., 2003, *A&A*, 401, 215
 Stanimirović, S., Weisberg, J. M., Hedden, A., Devine, K. E. & Green, J. T., 2003, *ApJ*, 598, L23
 van Ommen, T. D., Jones, D. L., Preston, R. A. & Jauncey, D. L., 1995, *ApJ*, 444, 561
 Wiklind, T. & Combes, F., 1996, *Nature*, 379, 139
 Wiklind, T. & Combes, F., 1997, *A&A*, 328, 48
 Wiklind, T. & Combes, F., 1998, *ApJ*, 500, 129
 Wiklind, T. & Combes, F., 1999, *astro-ph/9909314*
 Williams, J. A., Dickel, H. R. & Auer, L. H., 2004, *ApJS*, 153, 463
 Winn, J. N., Kochanek, C. S., McLeod, B. A., et al., 2002, *ApJ*, 575, 103
 Wolfe, A. M., Briggs, F. H. & Davis, M. M., 1982, *ApJ*, 259, 495

Table 1. Observations of the HCO⁺ (2-1) absorption line.

Date	Julian Day	Telescope	Total flux \diamond (Jy)	NE/SW flux ratio \diamond	$\int \tau dV$ (NE) \dagger (km s ⁻¹)	$\int \tau dV$ (SW blue) \dagger (km s ⁻¹)
1995 Sep 30	2449991	PdBI	–	1.51 (0.20)	2.28 (–)	14.40 (–)
1995 Oct 28	2450017	PdBI	–	1.78 (0.20)	2.51 (–)	13.32 (–)
1996 May 01	2450205	30m	1.2	1.87 (0.19)	0.62 (0.78)	8.17 (1.64)
1996 May 25	2450229	30m	1.1	1.84 (0.10)	1.93 (0.41)	10.82 (0.84)
1996 Jun 06	2450241	30m	0.8	3.13 (0.26)	1.23 (0.43)	15.29 (1.53)
1996 Jun 13	2450248	30m	1.0	1.89 (0.15)	2.43 (0.60)	13.42 (1.27)
1996 Jun 23	2450258	30m	1.0	1.79 (0.06)	2.85 (0.24)	11.09 (0.47)
1996 Jun 29	2450264	30m	1.0	1.65 (0.09)	2.28 (0.46)	15.20 (0.84)
1996 Jul 06	2450271	30m	1.1	2.99 (0.29)	1.27 (0.51)	5.66 (1.78)
1996 Jul 14	2450279	30m	0.9	1.52 (0.10)	2.43 (0.56)	15.79 (0.94)
1996 Jul 19	2450284	30m	0.9	1.50 (0.10)	2.56 (0.54)	10.65 (0.90)
1996 Jul 23	2450288	30m	1.0	1.71 (0.12)	0.69 (0.57)	7.02 (1.09)
1996 Aug 04	2450300	30m	1.0	1.63 (0.07)	2.99 (0.35)	14.02 (0.64)
1996 Aug 10	2450306	30m	1.2	2.18 (0.12)	1.37 (0.36)	7.26 (0.88)
1996 Aug 19	2450315	30m	1.1	1.73 (0.07)	1.66 (0.31)	8.28 (0.60)
1996 Aug 25	2450321	30m	1.0	1.75 (0.04)	1.99 (0.16)	10.89 (0.30)
1996 Sep 01	2450328	30m	1.1	1.38 (0.06)	1.33 (0.39)	10.12 (0.59)
1996 Sep 16	2450343	30m	0.8	1.08 (0.10)	2.23 (0.93)	11.42 (1.12)
1996 Sep 20	2450347	30m	0.8	1.9 (0.14)	3.44 (0.54)	16.10 (1.13)
1996 Sep 24	2450351	30m	1.0	2.19 (0.10)	2.30 (0.32)	10.62 (0.78)
1996 Oct 28	2450385	30m	0.9	1.37 (0.06)	2.46 (0.38)	9.47 (0.58)
1996 Nov 07	2450395	30m	0.9	1.55 (0.08)	2.13 (0.46)	10.94 (0.79)
1996 Nov 22	2450410	30m	0.9	1.77 (0.11)	3.59 (0.46)	12.51 (0.90)
1996 Nov 29	2450417	30m	0.9	1.64 (0.09)	1.49 (0.44)	8.94 (0.79)
1997 Apr 04	2450543	30m	1.0	1.83 (0.09)	0.64 (0.38)	10.74 (0.78)
1997 Apr 05	2450544	30m	0.9	1.7 (0.08)	2.39 (0.35)	11.34 (0.67)
1997 May 18	2450587	30m	1.2	1.65 (0.05)	1.23 (0.25)	9.32 (0.45)
1997 Jun 13	2450613	30m	1.2	1.55 (0.06)	1.20 (0.33)	10.64 (0.58)
1997 Jun 28	2450628	30m	1.3	1.64 (0.07)	1.63 (0.32)	10.25 (0.59)
1997 Jul 10	2450640	30m	1.2	1.48 (0.04)	1.86 (0.25)	9.45 (0.41)
1997 Jul 13	2450643	30m	0.8	0.98 (0.09)	2.62 (1.06)	8.85 (1.15)
1997 Aug 09	2450670	30m	1.2	1.85 (0.12)	1.41 (0.49)	13.34 (1.01)
1997 Aug 12	2450673	30m	1.2	1.56 (0.07)	2.09 (0.38)	10.29 (0.66)
1997 Aug 13	2450674	30m	1.1	1.79 (0.19)	-0.06 (0.82)	10.49 (1.63)
1997 Aug 15	2450676	30m	1.1	1.54 (0.10)	1.28 (0.52)	11.27 (0.88)
1997 Aug 16	2450677	30m	1.1	1.49 (0.20)	0.95 (1.15)	5.49 (1.94)
1997 Aug 19	2450680	30m	1.1	1.8 (0.13)	1.91 (0.55)	7.14 (1.09)
1997 Aug 22	2450683	30m	1.2	1.53 (0.09)	1.54 (0.48)	11.31 (0.81)
1997 Aug 26	2450687	30m	1.2	1.85 (0.10)	2.06 (0.41)	9.30 (0.85)
1997 Aug 30	2450691	30m	1.5	2.05 (0.11)	1.76 (0.37)	10.48 (0.83)
1997 Sep 03	2450695	30m	1.2	2.07 (0.08)	2.00 (0.27)	8.79 (0.62)
1997 Sep 06	2450698	30m	1.4	1.85 (0.10)	0.91 (0.39)	7.02 (0.80)
1997 Sep 10	2450702	30m	1.4	1.75 (0.07)	2.00 (0.29)	8.82 (0.57)
1997 Sep 16	2450708	30m	1.4	1.67 (0.10)	3.14 (0.48)	12.44 (0.90)
1997 Sep 26	2450718	30m	1.1	1.31 (0.07)	2.33 (0.52)	10.81 (0.76)
1997 Oct 03	2450725	30m	1.4	1.48 (0.07)	1.62 (0.42)	12.15 (0.68)
1997 Oct 18	2450740	30m	1.4	1.37 (0.05)	2.25 (0.31)	10.28 (0.48)
1998 Dec 25	2451173	30m	2.2	1.50 (0.07)	3.53 (0.38)	16.59 (0.62)
1999 Jan 02	2451181	30m	1.6	1.55 (0.04)	3.35 (0.23)	17.63 (0.40)
1999 Jan 11	2451190	30m	1.9	1.61 (0.05)	2.97 (0.25)	15.09 (0.45)
1999 Jan 27	2451206	30m	2.2	1.51 (0.06)	2.48 (0.31)	14.36 (0.53)
1999 Jan 30	2451209	30m	2.2	1.51 (0.06)	3.17 (0.34)	14.73 (0.56)
1999 Apr 23	2451292	30m	2.0	1.43 (0.04)	6.01 (0.23)	20.75 (0.37)
1999 May 05	2451304	30m	2.1	1.98 (0.09)	4.27 (0.34)	17.91 (0.75)
1999 May 12	2451311	30m	2.0	1.63 (0.04)	5.37 (0.20)	22.22 (0.36)
1999 Jun 11	2451341	PdBI	2.3	1.64 (0.02)	5.6 (0.08)	22.77 (0.14)
1999 Jun 13	2451343	30m	2.0	1.64 (0.05)	5.64 (0.24)	22.36 (0.43)
1999 Jun 18	2451348	30m	2.1	1.53 (0.04)	4.70 (0.23)	21.34 (0.39)
1999 Jul 09	2451369	30m	1.9	1.39 (0.04)	6.07 (0.23)	22.31 (0.35)
1999 Jul 23	2451383	30m	1.9	1.48 (0.04)	5.81 (0.23)	25.36 (0.38)
1999 Jul 30	2451390	30m	1.8	1.43 (0.04)	5.70 (0.27)	24.37 (0.43)
2001 Mar 20	2451989	PdBI	2.4	1.52 (0.02)	4.83 (0.10)	22.76 (0.17)
2001 Jun 29	2452090	PdBI	2.9	1.58 (0.01)	5.76 (0.07)	24.81 (0.12)
2002 Jun 25	2452451	PdBI	2.4	1.68 (0.04)	4.75 (0.17)	20.78 (0.32)
2003 Feb 26	2452697	PdBI	1.7	1.72 (0.03)	3.78 (0.14)	15.10 (0.26)
2003 Mar 01	2452700	PdBI	1.8	1.60 (0.03)	3.59 (0.14)	16.93 (0.25)
2006 May 20	2453876	PdBI	2.4	1.37 (0.03)	1.11 (0.19)	9.68 (0.27)
2006 Jul 17	2453934	PdBI	1.7	1.71 (0.03)	1.49 (0.13)	11.81 (0.23)